

# Dynamical second-order noise sweetspots in resonantly driven spin qubits

Jordi Picó-Cortés<sup>1,2</sup> and Gloria Platero<sup>1</sup>

<sup>1</sup>Instituto de Ciencia de Materiales de Madrid (CSIC) 28049, Madrid, Spain.

<sup>2</sup>Institute for Theoretical Physics, University of Regensburg, 93040 Regensburg, Germany.

Quantum dot-based quantum computation employs extensively the exchange interaction between nearby electronic spins in order to manipulate and couple different qubits. The exchange interaction, however, couples the qubit states to charge noise, which reduces the fidelity of the quantum gates that employ it. The effect of charge noise can be mitigated by working at noise sweetspots in which the sensitivity to charge variations is reduced. In this work we study the response to charge noise of a double quantum dot based qubit in the presence of ac gates, with arbitrary driving amplitudes, applied either to the dot levels or to the tunneling barrier. Tuning with an ac driving allows to manipulate the sign and strength of the exchange interaction as well as its coupling to environmental electric noise. Moreover, we show the possibility of inducing a second-order sweetspot in the resonant spin-triplet qubit in which the dephasing time is significantly increased.

## 1 Introduction

Quantum computation in quantum dot arrays makes extensive use of the exchange interaction between the electron spins both for one[1, 2] and two-qubit gates[3, 4]. Unfortunately, the exchange interaction couples the qubit states to electric noise due to fluctuations in the charging energy[5, 6], defects in the dot[7, 8] and the interaction with the electric environment[9] resulting in reduced coherence times[10, 11]. Moreover, the exchange interaction may result in double occupancy [12, 13] and leakage errors[14–16]. Nonetheless, it has been employed to reach large gate fidelities in quantum dot-based qubits[17, 18] and forms the basis of an extending number of proposals for solid state quantum computation[19–24].

One promising venue for improvement is the use of ac gates in order to tune the properties of the quan-

Jordi Picó-Cortés: [Jordi.Pico-Cortes@physik.uni-regensburg.de](mailto:Jordi.Pico-Cortes@physik.uni-regensburg.de)

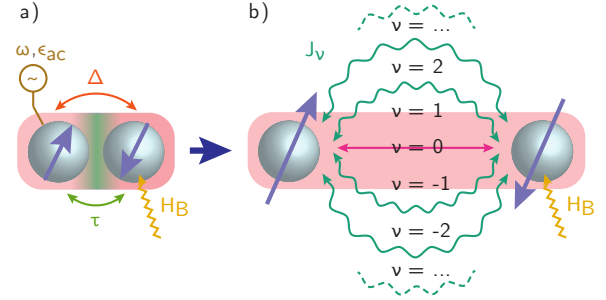


Figure 1: a) Scheme of the system. A DQD with a single electron spin defined in each dot and a tunneling amplitude  $\tau$  between both is set under a magnetic field gradient  $\Delta$ . The leftmost dot is subjected to an ac gate of amplitude  $\epsilon_{ac}$  and frequency  $\omega$ . The system is coupled to a bosonic bath  $\hat{H}_B$ , denoted by a yellow arrow, accounting for the effect of charge noise. b) Scheme of the exchange interaction with an ac field included. The different sidebands (marked in green) correspond to processes involving the absorption or emission of a photon and together contribute to the total exchange rate.

tum dot array[25, 26], in what has been termed Floquet engineering[27–30] of quantum systems. In the presence of ac gates, electron tunneling is accompanied by the absorption or emission of photons, resulting in a new set of photoassisted paths, called sidebands[31, 32]. The exchange interaction, as a virtual tunneling process, is similarly modified by the ac driving[33, 34]. Several qubit platforms employing a resonant exchange interaction have been studied both theoretically and experimentally[35–38]. Resonant exchange qubits based on double quantum dots in both GaAs/AlGaAs heterostructures[39] and Silicon[40], as well as on triple quantum dots[41, 42] have been developed. The latter allows for qubit operation involving only the exchange interaction and show excellent protection against electric noise[43]. Similarly, resonant exchange CNOT gates have been developed and implemented experimentally which employ the same method of operation[44, 45].

In the recent years, several works[46–50] have devel-

oped the idea of employing ac gates to engineer noise sweetspots[51, 52] in which the decoherence time due to noise is significantly increased. A recent paper[53] shows how an ac voltage can induce a dynamical sweetspot due to sideband interference, suppressing the coupling to the electric environment. In this work, we study how to employ ac gates to induce dynamical sweetspots in a qubit defined on a double quantum dot (DQD). The DQD qubit is an ideal platform to analyze dynamical sweetspots in the photoassisted exchange interaction both for its simplicity and because electric noise is often the most important source of decoherence, in particular for purified silicon[54, 55]. The DQD-based resonant qubit is operated by tuning the frequency of the oscillating exchange interaction in resonance with the splitting between the  $|\uparrow, \downarrow\rangle, |\downarrow, \uparrow\rangle$  states due to a magnetic field gradient. We consider the effect of modulating both the dot gates and the tunneling barriers with an ac voltage, and investigate resonances involving an arbitrary number of photons. Moreover, we show how an ac gate can be used to engineer the coupling between the electric environment and the DQD. In particular, when driven with a particular amplitude of the ac gate, we find that the DQD exhibits a second-order sweetspot[56] in which the qubit is unaffected by noise up to second order in the coupling with the electric environment, significantly increasing the dephasing time of the qubit.

The paper is organized as follows. In Sec. 2 we introduce the theoretical model that we will be employing. In Sec. 3.1 the basic features of the qubit operation are introduced. In particular, we consider the case of a resonant transition between the two  $S_z = 0$  states with one unpaired spin in each dot mediated by the ac voltage. In Sec. 3.2 we explore the different ways in which the ac gate can be used to improve the qubit operation under charge noise for the cases where the ac gate voltages are applied to the individual quantum dots and to the tunneling gates between them, respectively. Finally, in Sec. 4 we summarize the results and discuss the experimental implementation of the proposal.

## 2 Theoretical Model

We consider the Hamiltonian for a DQD in an extended Hubbard model with nearest neighbor tunneling  $\tau$  between the two sites, denoted by  $\alpha = 1, 2$ , Zeeman splittings  $E_{z,\alpha}$ , and both intra-dot and inter-dot interactions,  $U_\alpha$  and  $V$  respectively. The dot in the left is subjected to an ac voltage of amplitude  $\epsilon_{ac}$ , frequency  $\omega$ , and with an initial phase  $\phi$ . The Hamiltonian governing the DQD dynamics is then given by

$$\begin{aligned}\hat{H}(t) &= \hat{H}_0 + \hat{H}_{ac}(t) + \hat{H}_U + \hat{H}_T, \\ \hat{H}_0 &= \sum_{\alpha;\sigma} \epsilon_\alpha \hat{n}_{\alpha,\sigma} + \sum_{\alpha} \hbar^{-1} E_{z,\alpha} \hat{S}_{z,\alpha}, \\ \hat{H}_U &= \sum_{\alpha} U_\alpha \hat{n}_{\alpha,\uparrow} \hat{n}_{\alpha,\downarrow} + \sum_{\alpha < \beta; \sigma, \sigma'} V \hat{n}_{\alpha,\sigma} \hat{n}_{\beta,\sigma'}, \\ \hat{H}_T &= \sum_{\alpha, \beta; \sigma} \tau (\hat{c}_{\alpha,\sigma}^\dagger \hat{c}_{\beta,\sigma} + \text{H.c.}),\end{aligned}\tag{1}$$

where  $\hat{c}_{\alpha,\sigma}^\dagger$  ( $\hat{c}_{\alpha,\sigma}$ ) is the fermion creation (annihilation) operator for an electron in dot  $\alpha$  with spin  $\sigma = \uparrow, \downarrow$  and  $\hat{n}_{\alpha,\sigma} = \hat{c}_{\alpha,\sigma}^\dagger \hat{c}_{\alpha,\sigma}$ . The ac gates can be introduced either as a quantum dot gate  $\hat{H}_{ac}(t) = \sum_{\sigma} \epsilon_{ac} \hat{n}_{1,\sigma} \cos(\omega t + \phi)$  or in the tunneling amplitude as<sup>1</sup>  $\hat{H}_{ac}(t) = (\tau_{ac}/\tau) \cos(\omega t + \phi) \hat{H}_T$ . In actual experimental conditions, both are expected to be present[57] as they appear as a result of modulations of the same interconnected potential. We will consider them separately here for reasons of simplicity. The DQD with all processes in Eq. 1 is represented schematically in Fig. 1 a).

Considering that the DQD can be occupied by a maximum of two electrons, the relevant states have either spin projection  $|S_z| = 1$ ,  $\{|\uparrow, \uparrow\rangle, |\downarrow, \downarrow\rangle\}$  or  $S_z = 0$ , including the two qubit states  $\mathcal{Q} = \{|\uparrow, \downarrow\rangle, |\downarrow, \uparrow\rangle\}$  and two states with double occupancy,  $\mathcal{D} = \{|\uparrow\downarrow, 0\rangle, |0, \uparrow\downarrow\rangle\}$ , where  $|\sigma, \sigma'\rangle$  is the state with spin  $\sigma$  in the left dot and spin  $\sigma'$  in the right dot. The two states with  $|S_z| = 1$ , are not connected to the rest by any term in the ideal Hamiltonian of Eq. 1. In realistic conditions, the  $S_z = 0$  and the  $|S_z| = 1$  subspaces are connected through coupling to the environment, including the nuclear spin bath coupled through the hyperfine interaction and phonons coupled through the spin-orbit interaction or magnetic field gradients. We will consider that the qubit is operated in a time scale shorter than the relaxation, leakage and dephasing times associated with these processes—which can be quite large for isotopically purified Silicon[54, 55] or if spin-echo sequences are used[58, 59]—and focus on the  $S_z = 0$  subspace. However, Silicon carries its own complications in the form of valley physics[60, 61]. The valley splitting in Silicon can nonetheless be tuned by the use of gate potentials resulting in high inter-valley relaxation lifetimes[62, 63].

<sup>1</sup>The dependence of the tunneling amplitude on the gate voltage may also be non-trivial[44], resulting in higher harmonics in  $\tau(t)$  and the possibility of resonances involving a higher number of photons.

### 3 Results

#### 3.1 Qubit operation with ac gates

The qubit, consisting of the states  $|\uparrow, \downarrow\rangle$  and  $|\downarrow, \uparrow\rangle$ , is initialized in the ground state of the static qubit. The ac bias is then tuned to the resonance frequency between the qubit states. Initialization can be performed adiabatically in order to ensure that the dressed states are mapped correctly from the static eigenstates[49, 64, 65]. Similarly, readout can be performed by adiabatically turning off the ac voltage. The physics in the resonance can be studied in a convenient time-independent framework by employing an effective co-tunneling Hamiltonian in the Rotating Wave Approximation (RWA). We consider that the ac voltage is applied in the left quantum dot in a resonance involving  $n$  photons, but allow for a small offset of the resonance (compared to the ac voltage frequency). Then, the qubit Hamiltonian can be written as (See Appendix A)

$$\hat{H}_Q^{(0)} = (\Delta E - n\hbar\omega) \hat{\sigma}_z + \mathcal{J}_n \cos(n\phi) \hat{\sigma}_x + \mathcal{J}_n \sin(n\phi) \hat{\sigma}_y, \quad (2)$$

where  $\hat{\sigma}_k$ ,  $k = x, y, z$  are the Pauli matrices in the basis  $\{|\uparrow, \downarrow\rangle, |\downarrow, \uparrow\rangle\}$  and

$$\begin{aligned} \Delta E &= E^+ - E^-, \\ E^\pm &= \pm \Delta \\ &- 2\tau^2 \sum_{\nu=-\infty}^{\infty} \left[ \frac{J_\nu^2\left(\frac{\epsilon_{ac}}{\hbar\omega}\right)}{\delta_2 \mp \Delta - \nu\hbar\omega} + \frac{J_\nu^2\left(\frac{\epsilon_{ac}}{\hbar\omega}\right)}{\delta_1 \mp \Delta + \nu\hbar\omega} \right], \end{aligned} \quad (3)$$

$$\begin{aligned} \mathcal{J}_n &= \tau^2 \sum_{\nu=-\infty}^{\infty} \\ &\times \left[ \frac{J_\nu\left(\frac{\epsilon_{ac}}{\hbar\omega}\right) J_{\nu-n}\left(\frac{\epsilon_{ac}}{\hbar\omega}\right)}{\delta_1 - \Delta + \nu\hbar\omega} + \frac{J_\nu\left(\frac{\epsilon_{ac}}{\hbar\omega}\right) J_{\nu-n}\left(\frac{\epsilon_{ac}}{\hbar\omega}\right)}{\delta_2 + \Delta - \nu\hbar\omega} \right. \\ &\left. + \frac{J_\nu\left(\frac{\epsilon_{ac}}{\hbar\omega}\right) J_{\nu+n}\left(\frac{\epsilon_{ac}}{\hbar\omega}\right)}{\delta_2 - \Delta - \nu\hbar\omega} + \frac{J_\nu\left(\frac{\epsilon_{ac}}{\hbar\omega}\right) J_{\nu+n}\left(\frac{\epsilon_{ac}}{\hbar\omega}\right)}{\delta_1 + \Delta + \nu\hbar\omega} \right]. \end{aligned} \quad (4)$$

Here,  $J_\nu(z)$  is the  $\nu$ th Bessel function of the first kind,  $\Delta = E_{z,1} - E_{z,2}$ ,  $\delta_0 = \epsilon_2 - \epsilon_1$ ,  $\delta_1 = U_1 - V - \delta_0$  and  $\delta_2 = U_2 - V + \delta_0$ , corresponding to the gradient splitting, the detuning between the dot levels and the energy difference between the  $S_z = 0$  states with (1,1) occupation and the ones with (2,0) and (0,2), respectively. The qubit defined in Eq. 2 can be controlled by a proper alignment of the ac field phase  $\phi$ . Alternatively, it can be operated by varying the gate parameter  $\delta_0 = \epsilon_2 - \epsilon_1$  or the tunneling amplitude  $\tau$ [66] employing the same techniques as for the regular static qubit.

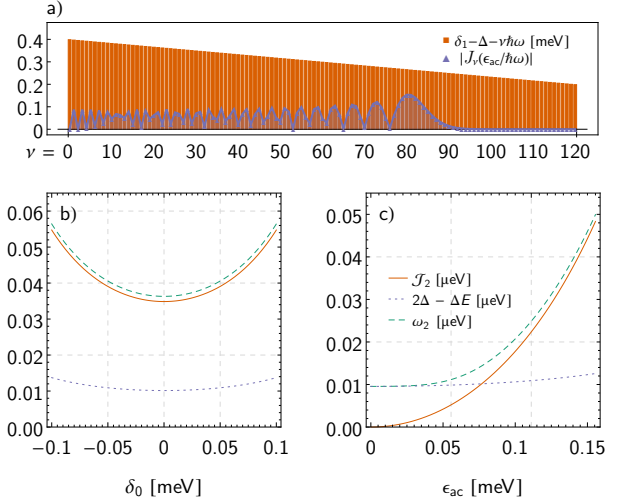


Figure 2: a) In red bars, the energy difference between  $|\uparrow, \downarrow\rangle$  and  $|\downarrow, \uparrow, 0\rangle$  (i.e., the lowest contribution to the denominators in Eqs. 4 and 5) for each sideband transition  $\nu$  at  $\delta_0 = 0$ . In blue lines, the absolute value of the corresponding Bessel function  $J_\nu(\epsilon_{ac}/\hbar\omega)$  for  $\epsilon_{ac} = 0.14$  meV at the  $n = 2$  resonance (see text). For  $\nu \simeq 120$  the Bessel functions are negligible, far from the photoassisted resonance, indicating that the system is properly described including up to this value. b) The exchange interaction  $\mathcal{J}_2$  (red, continuous), the correction to the energy splitting  $\Delta - \Delta E$  (blue, dotted), and the qubit energy  $\omega_2 = \sqrt{\mathcal{J}_2^2 + (\Delta E - 2\hbar\omega)^2}$  (green, dashed, see text) as a function of  $\delta_0$  at  $\epsilon_{ac} = 0.14$  meV. c) The same three quantities as a function of the ac voltage amplitude  $\epsilon_{ac}$  at  $\delta_0 = 0.085$  meV. Parameters employed:  $\Delta = 1.666$   $\mu$  eV,  $U_1 = U_2 = 0.5$  meV,  $V = 0.1$  meV,  $\tau = 0.01$  meV, and  $\hbar\omega = \Delta$ .

The physical origin of the energy splitting  $\Delta E$  is as follows: a magnetic field gradient reduces (increases) the energy difference between  $|\downarrow, \uparrow\rangle$  ( $|\uparrow, \downarrow\rangle$ ) and the doubly occupied states  $\{|\uparrow\downarrow, 0\rangle, |0, \uparrow\downarrow\rangle\}$ . As a result, the perturbative transition rate between  $|\downarrow, \uparrow\rangle$  ( $|\uparrow, \downarrow\rangle$ ) and the doubly occupied states is increased (reduced). This is reflected at second order of the perturbation as a reduction of the energy splitting. The other term appearing in Eq. 2 is the (resonant) exchange interaction, which corresponds to transitions between  $|\uparrow, \downarrow\rangle$  and  $|\downarrow, \uparrow\rangle$  due to virtual tunneling processes through  $\mathcal{D}$ . These are represented both as a function of  $\delta_0$  and  $\epsilon_{ac}$  in Fig. 2 b) and c), respectively.

Estimating the range of validity of these expressions is particularly difficult in the high voltage amplitude  $\epsilon_{ac}/\hbar\omega \gg 1$  regime. Since the sideband strength is governed by  $J_\nu(\epsilon_{ac}/\hbar\omega)$ , there is a large number of active sidebands in this regime. Moreover, because  $\hbar\omega \sim |\Delta| \ll |\delta_1|, |\delta_2|$ , there is a certain  $\tilde{\nu}$  for which at least one denominator in Eqs. 4 and 5 will be zero or very close to it (i.e.  $\delta_k \pm \Delta \pm \tilde{\nu}\hbar\omega \simeq 0$ ,  $k = 1, 2$ ).

This corresponds to a photoassisted resonance with the doubly occupied states and the perturbative expansion fails. For that reason, we consider ac voltage amplitudes that are small enough that we can neglect photoassisted transitions to  $\mathcal{D}$ . This is the case provided that  $\tau^2 J_\nu^2 (\epsilon_{ac}/\hbar\omega) (\delta_k \pm \Delta \pm \nu\hbar\omega)^{-1} \ll \Delta E, \mathcal{J}_n$ , with  $k = 1, 2$ . In particular, in Appendix C we discuss the limit of  $\epsilon_{ac} \ll \hbar\omega$ , where the expressions of Eqs. 4 and 5 have simple forms. This is represented schematically in Fig. 2 a) where we have plotted the minimum of the denominators of Eqs. 4 and 5 for each sideband, as well as the corresponding Bessel function. Above a certain  $\nu$  (around 40 in this case, quite smaller than  $\tilde{\nu}$  for  $\delta_0 \simeq 0$ ) the sidebands can be neglected and the cotunneling approximation is valid (See Appendix B).

Another possible route to manipulate the qubit is by employing an ac driving in the tunneling amplitude. From the choice of gate described below Eq. 1, this corresponds to replacing  $J_\nu (\epsilon_{ac}/\hbar\omega)$  by  $\tau_\nu$  in Eqs. 15-16 of the appendix, where  $\tau_\nu = \delta_{\nu 0}\tau + \delta_{|\nu|,1}\tau_{ac}/2$ . For this simple choice of the tunneling amplitude, only resonances with one or two photons yield a time-independent Hamiltonian like Eq. 2. For  $n = 1$  (single-photon resonance) we have

$$\begin{aligned} \Delta E = 2\Delta - \tau^2 & \left[ \frac{2\Delta}{\delta_2^2 - \Delta^2} + \frac{2\Delta}{\delta_1^2 - \Delta^2} \right] \\ & - \frac{\tau_{ac}^2}{2} \left[ \frac{\Delta + \hbar\omega}{\delta_2^2 - (\Delta + \hbar\omega)^2} + \frac{\Delta + \hbar\omega}{\delta_1^2 - (\Delta + \hbar\omega)^2} \right] \\ & - \frac{\tau_{ac}^2}{2} \left[ \frac{\Delta - \hbar\omega}{\delta_2^2 - (\Delta - \hbar\omega)^2} + \frac{\Delta - \hbar\omega}{\delta_1^2 - (\Delta - \hbar\omega)^2} \right], \end{aligned} \quad (6)$$

$$\begin{aligned} \mathcal{J}_1 = \tau\tau_{ac} & \left[ \frac{\delta_1}{\delta_1^2 - \Delta^2} + \frac{\delta_2}{\delta_2^2 - \Delta^2} \right. \\ & \left. + \frac{\delta_1}{\delta_1^2 - (\Delta - \hbar\omega)^2} + \frac{\delta_2}{\delta_2^2 - (\Delta - \hbar\omega)^2} \right]. \end{aligned} \quad (7)$$

For  $n = 2$  (two-photons resonance) the exchange interaction is

$$\mathcal{J}_2 = \frac{\tau_{ac}^2}{2} \left[ \frac{\delta_1}{\delta_1^2 - (\Delta - \hbar\omega)^2} + \frac{\delta_2}{\delta_2^2 - (\Delta - \hbar\omega)^2} \right]. \quad (8)$$

### 3.2 Operation under electric noise

When operating the qubit, the DQD is subjected to electric noise coupling to the Hamiltonian of Eq. 2 through the dependence of  $\Delta E$  and  $\mathcal{J}_n$  on  $\delta_{1,2}, \tau$ , and on  $\epsilon_{ac}$  or  $\tau_{ac}$ . This results in a loss of coherence during qubit operation. The noisy environment can be characterized by the spectral density which we assume has

the form [67, 68]  $\mathcal{S}(\Omega) = A/|\Omega|$ , often called  $1/f$  noise. Following Ref. [69], we will consider both infrared  $\Omega_{IR}$  and ultraviolet  $\Omega_{UV}$  cutoffs in  $\mathcal{S}(\Omega)$  for low and high frequencies, respectively.

In this work, we focus on the effect of charge noise entering through the on-site energy of the dots, resulting in fluctuations of the parameter  $\delta_0$ . Nonetheless, the same techniques described below can be employed with other sources of electric noise. We consider the effect of noise in the context of a Ramsey-like decay [70, 71]. The dephasing time can then be estimated as [69]

$$\begin{aligned} T_\varphi^{-2} = & \frac{A}{2\hbar^2} \left( \frac{\partial\omega_n}{\partial\delta_0} \right)^2 \log \gamma \\ & + \frac{A^2}{4\hbar^2} \left( \frac{\partial^2\omega_n}{\partial\delta_0^2} \right)^2 \log^2 \gamma + \mathcal{O}(A^3), \end{aligned} \quad (9)$$

where  $\gamma = \Omega_{UV}/\Omega_{IR}$  and we have defined the qubit energy  $\omega_n = \sqrt{\mathcal{J}_n^2 + (\Delta E - n\hbar\omega)^2}$ , corresponding to half of the energy splitting between the two eigenstates of the diagonalized Hamiltonian  $\hat{H}_Q^{(0)}$ . This expression is obtained in the context of the time-independent RWA Hamiltonian, Eq. 2, but the terms neglected in the RWA approximation do not contribute significantly to dephasing in the high frequency regime. In particular, in Appendix E we consider the contribution to the dephasing due to the neglected sidebands and show that they do not yield an exponential decay of the coherence for times larger than  $\omega^{-1}$ .

Since  $A$  is often a small scale of the system, the first-order susceptibility  $\partial\omega_n/\partial\delta_0$  is of particular importance. The points at which  $\partial\omega_n/\partial\delta_0 = 0$  are *first-order sweetspots*, where the dephasing time is infinite up to first order in  $A$ . Similarly, the points where  $\partial\omega_n^2/\partial\delta_0^2 = 0$  is also zero are *second-order sweetspots* and the dephasing time is infinite up to second order in  $A$ . Higher order sweetspots are also possible [72] for configurations beyond the scope of this work.

For the undriven DQD-based qubit, there exists a first-order sweetspot at  $\delta_1 = \delta_2$ . At this point, the virtual transitions to  $|\uparrow\downarrow, 0\rangle$  and  $|0, \uparrow\downarrow\rangle$  interfere in such a way that the first-order susceptibility is zero. This is still true in the ac-driven qubit. In particular, for arbitrary  $n$ , we have at  $\delta_1 = \delta_2$

$$\begin{aligned}
\left. \frac{\partial \Delta E}{\partial \delta_0} \right|_{\delta_1=\delta_2} &= 0, \\
\left. \frac{\partial \mathcal{J}_n}{\partial \delta_0} \right|_{\delta_1=\delta_2} &= \tau^2 [(-1)^n - 1] \\
&\times \left[ \sum_{\nu=1}^{\infty} J_{\nu} \left( \frac{\epsilon_{ac}}{\hbar\omega} \right) J_{\nu+n} \left( \frac{\epsilon_{ac}}{\hbar\omega} \right) \frac{4\delta_1 (\Delta + \nu\hbar\omega)}{[\delta_1^2 - (\Delta + \nu\hbar\omega)^2]^2} \right. \\
&\left. - \sum_{\nu=0}^{\infty} J_{\nu} \left( \frac{\epsilon_{ac}}{\hbar\omega} \right) J_{\nu-n} \left( \frac{\epsilon_{ac}}{\hbar\omega} \right) \frac{4\delta_1 (\Delta - \nu\hbar\omega)}{[\delta_1^2 - (\Delta - \nu\hbar\omega)^2]^2} \right]. \quad (11)
\end{aligned}$$

$$\left. \frac{\partial \omega_n}{\partial \delta_0} \right|_{\delta_1=\delta_2} = \frac{\mathcal{J}_n}{\omega_n} \left. \frac{\partial \mathcal{J}_n}{\partial \delta_0} \right|_{\delta_1=\delta_2}. \quad (12)$$

For even  $n$ ,  $\partial \mathcal{J}_n / \partial \delta_0 = \partial \omega_n / \partial \delta_0 = 0$  at  $\delta_1 = \delta_2$ , as can be seen from the prefactor in the expression for  $\partial \mathcal{J}_n / \partial \delta_0$ . That is: the sweetspot in the static qubit survives to the dynamic case. For odd  $n$ , on the other hand,  $\mathcal{J}_n = 0$  at  $\delta_1 = \delta_2$ , and therefore  $\partial \omega_n / \partial \delta_0$  is also zero at this point. Hence, while there is also a first-order sweetspot for odd  $n$  at  $\delta_1 = \delta_2$ , the exchange interaction is zero at it, rendering this point useless for operating the qubit. In general, for arbitrary  $n$ , we have

$$\begin{aligned}
\mathcal{J}_n|_{\delta_1=\delta_2} &= \tau^2 \delta_1 [(-1)^n + 1] \\
&\times \left[ \sum_{\nu=0}^{\infty} \frac{J_{\nu} \left( \frac{\epsilon_{ac}}{\hbar\omega} \right) J_{\nu+n} \left( \frac{\epsilon_{ac}}{\hbar\omega} \right)}{\delta_1^2 - (\Delta + \nu\hbar\omega)^2} \right. \\
&\left. + \sum_{\nu=1}^{\infty} \frac{J_{\nu} \left( \frac{\epsilon_{ac}}{\hbar\omega} \right) J_{\nu-n} \left( \frac{\epsilon_{ac}}{\hbar\omega} \right)}{\delta_1^2 - (\Delta - \nu\hbar\omega)^2} \right], \quad (13)
\end{aligned}$$

We have represented  $\mathcal{J}_1$ , the correction to the energy splitting  $2\Delta - \Delta E$  and  $\omega_1$  in Fig. 3 a) as a function of  $\delta_0$  and for  $n = 1$ . Note that since  $\mathcal{J}_1$  changes sign as it crosses  $\delta_0 = 0$  (corresponding to  $\delta_1 = \delta_2$  in the symmetric configuration  $U_1 = U_2$ ), a combined manipulation of the ac and dc gates can be employed to reverse the ground state of the singlet-triplet qubit, enabling initialization in the triplet subspace (in the rotating frame). Fig. 3 b) shows the first-order derivatives  $\partial_{\delta_0} X$ ,  $X = \mathcal{J}_1, \Delta E$ , and  $\omega_1$  as a function of the ac voltage amplitude for  $\delta_0 = 0.07$  meV.

The first-order derivatives for  $n = 2$ ,  $\partial_{\delta_0} X$ ,  $X = \mathcal{J}_2, \Delta E, \omega_2$ , are represented in Fig. 4 a), showing the presence of a sweetspot at  $\delta_0 = 0$ . One particular benefit of employing the two-photons resonance is that the system can be kept at the first-order sweetspot while the ac gate can be employed to increase the strength of the exchange interaction, yielding faster operation times while still keeping the system at the sweetspot.

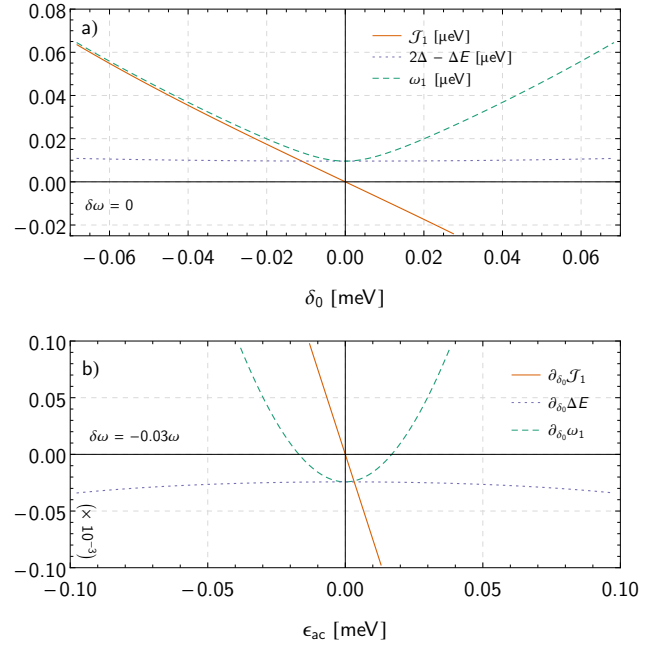


Figure 3: a) The exchange interaction  $\mathcal{J}_1$  (red, continuous), correction to the energy splitting  $2\Delta - \Delta E$  (blue, dotted), and qubit energy  $\omega_1 = \sqrt{\mathcal{J}_1^2 + (\Delta E - \hbar\omega)^2}$  (green, dashed) as a function of  $\delta_0$  at  $\epsilon_{ac} = 0.12$  meV with on-site driving. The exchange interaction is zero at  $\delta_0 = 0$ . b) First order derivative of the same three quantities as a function of  $\epsilon_{ac}$  for the same quantities and  $\delta_0 = 0.07$  meV. A first order sweetspot where  $\partial \omega_1 / \partial \delta_0 = 0$  is induced by the ac voltage at  $\epsilon_{ac} \simeq \pm 0.07$  meV. Same parameters as Fig. 2 with an offset of the resonance  $\delta\omega = -0.003\omega$  in b).

While this can certainly be beneficial for the qubit operation, fast operation requires larger ac voltage amplitudes ( $\propto \epsilon_{ac}^2$ ) than for  $n = 1$  ( $\propto \epsilon_{ac}$ ); moreover, the exchange for  $n$  even is  $\propto \Delta^2$ , compared to the  $n$  odd, which is  $\propto \Delta$  (See Appendix D).

Once at the sweetspot, the leading source of decoherence is through the second-order susceptibility  $\partial^2 \omega_n / \partial \delta_0^2$ . In the regular sweetspot  $\delta_1 = \delta_2$  for the static DQD qubit,  $\partial^2 \omega_n / \partial \delta_0^2 \neq 0$ , and the second-order contribution to dephasing is dominant. In the ac-driven DQD qubit, however, the second-order susceptibility can be zero for finite  $\epsilon_{ac}$ . For instance, consider the  $n = 2$  resonance at  $\delta_1 = \delta_2$ , so that  $\partial \mathcal{J}_2 / \partial \delta_0, \partial \Delta E / \partial \delta_0 = 0$ . Then, the second order susceptibility fulfills

$$\frac{\partial^2 \omega_2}{\partial \delta_0^2} = \frac{1}{\omega_2} \left[ \mathcal{J}_2 \frac{\partial^2 \mathcal{J}_2}{\partial \delta_0^2} + (\Delta E - 2\hbar\omega) \frac{\partial^2 \Delta E}{\partial \delta_0^2} \right]. \quad (14)$$

For a small offset of the resonance, such that  $\Delta E - 2\hbar\omega = \hbar\delta\omega$ , the contributions to  $\partial^2 \omega_2 / \partial \delta_0^2$  coming from  $\mathcal{J}_2$  and  $\Delta E$  have opposite sign and the susceptibility can



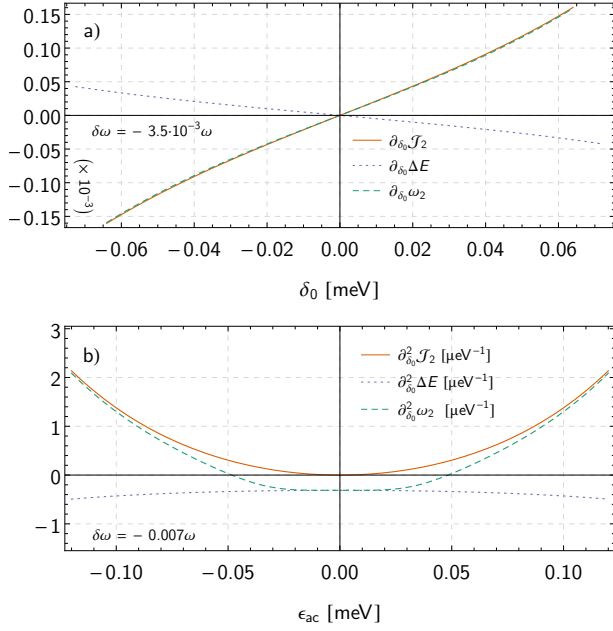


Figure 4: a) First and b) second order derivatives for the exchange interaction  $J_2$  (red, continuous), renormalized splitting  $\Delta E$  (blue, dotted) and the qubit splitting  $\omega_2$  (green, dashed) for the two photon ( $n = 2$ ) resonance as a function of  $\delta_2$  and  $\epsilon_{ac}$ , respectively, for the case of on-site driving. The dc sweetspot at  $\delta_0 = 0$  survives the presence of an ac voltage in this case, while there is a new dynamical second-order sweetspot where  $\partial^2 \omega_2 / \partial \delta_0^2 = 0$  at  $\epsilon_{ac} \simeq \pm 0.095$  meV. Same parameters as in Fig. 2 with an offset of the resonance  $\delta\omega = -0.007\omega$ .

be zero. This non-zero offset of the resonance does not break the conditions for the RWA provided that  $\delta\omega \ll \omega$ . Then, the ac voltage amplitude can be employed to tune the susceptibility to induce a second-order sweetspot. This renders the dephasing time infinite under the approximation of Eq. 9. In Fig. 4 b) we show an example of this for  $n = 2$ , where a second-order sweetspot can be obtained at  $\epsilon_{ac} \simeq 0.05$  meV. Similarly, for  $n = 1$  it is possible to find an easily accessible first-order dynamical sweetspot where  $\partial \omega_1 / \partial \delta_0 = 0$  for a small value of  $\epsilon_{ac}$ , as shown in Fig. 3 b).

Compared to the driving of the quantum dot gate voltage, driving the tunneling amplitude leads to an exchange interaction that does not vanish at  $\delta_1 = \delta_2$  for  $n = 1$  (and also does not change sign depending on  $\delta_0$ ). For  $n = 2$ ,  $\delta_1 = \delta_2$  is still a first-order sweetspot, while for  $n = 1$  this sweetspot is displaced to  $\delta_0 \neq 0$ . Following the same technique described in the previous section, the system can be tuned to induce a second-order sweetspot, using in this case the ac tunneling amplitude  $\tau_{ac}$ .

In Fig. 5 we represent the dephasing time for  $\gamma =$

$5 \cdot 10^6$  and  $A = 10^{-6}$  meV<sup>2</sup> (Figs. 5 a) - c)) and  $A = 10^{-4}$  meV<sup>2</sup> (Figs. 5 d) - f)), corresponding to the lower and upper bounds of the realistic range[43, 73]  $\sqrt{A} \sim 1 - 10$  μeV, respectively. From left to right, these are: the single-photon and two-photon resonances with the ac driving in the dot gates and the two-photon resonance with the ac driving in the tunneling gates. We have chosen an offset of the resonance condition that enables us to induce a first-order sweetspot for  $n = 1$  and a second-order sweetspot for the two configurations with  $n = 2$ .

For the case with the ac driving in the dot gates and  $n = 1$ , the exchange interaction is zero at  $\delta_0 = 0$ , as discussed above. Outside of  $\delta_0 = 0$ , in the arc around  $\epsilon_{ac} \simeq 15 - 18$  μeV (corresponding to the dynamical first-order sweetspot mentioned in Sec. 3.2), the dephasing time is still quite large,  $T_\varphi \sim 10^{-4}$  s for  $A = 10^{-6}$  meV<sup>2</sup> (Fig. 5 a)), compared with the typical Rabi period in this configuration ( $T_\Omega \sim 10^{-7}$  s). For a higher noise intensity (Fig. 5 d)), the region of long dephasing time corresponding to this dynamical sweetspot is less pronounced as the second-order contribution is more important. In the region close to the first-order dynamical sweetspot it is still possible to achieve a dephasing time of the order of  $10^{-3}$  s, but this decreases quickly as  $\delta_0$  is varied from zero. As a result, a compromise has to be reached between faster operation (moving away from  $\delta_0 = 0$ ) and increased dephasing time (moving closer to  $\delta_0 = 0$ ).

For  $n = 2$ , the intersection of  $\delta_0 = 0$  with  $\epsilon_{ac} \simeq 48$  μeV defines the second-order sweetspot discussed above, where the dephasing time is infinite under the dephasing model of Eq. 9 (i.e., up to terms  $\propto A^3$ ). For  $A = 10^{-6}$  meV<sup>2</sup> (Fig. 5 b)) the dephasing time is quite large ( $T_\varphi \sim 1 - 10$  ms) in the area around the sweetspot. The second-order sweetspot is still visible in Fig. 5 e), corresponding to higher noise intensity. However, while in Fig. 5 b)  $\delta_0 = 0$  corresponds to a region of longer dephasing time, in Fig. 5 e) the normal sweetspot has decreased in importance, while the dynamical sweetspot still yields large dephasing times even relatively far from  $\delta_0 = 0$ , showing the robustness of the dynamical sweetspot.

For the case of driving in the tunneling gate and  $n = 2$  (Fig. 5 c) and f)), as mentioned above, the first-order sweetspot is still at  $\delta_0 = 0$ , which can be seen clearly from the long dephasing time ( $T_\varphi \sim 10^{-5} - 10^{-4}$  s) in Fig. 5 c) and less so in Fig. 5 f) due to the higher noise intensity giving increased importance to the second-order term. Fig. 5 c) shows clearly a second-order sweetspot appearing at  $\tau_{ac} \simeq 5$  μeV, and  $\delta_0 = 0$ . Again, the results for stronger noise in Fig. 5 f) show the second-order sweetspot clearly. Interestingly, while the region of longer dephasing time at  $\delta_0 = 0$  is much less

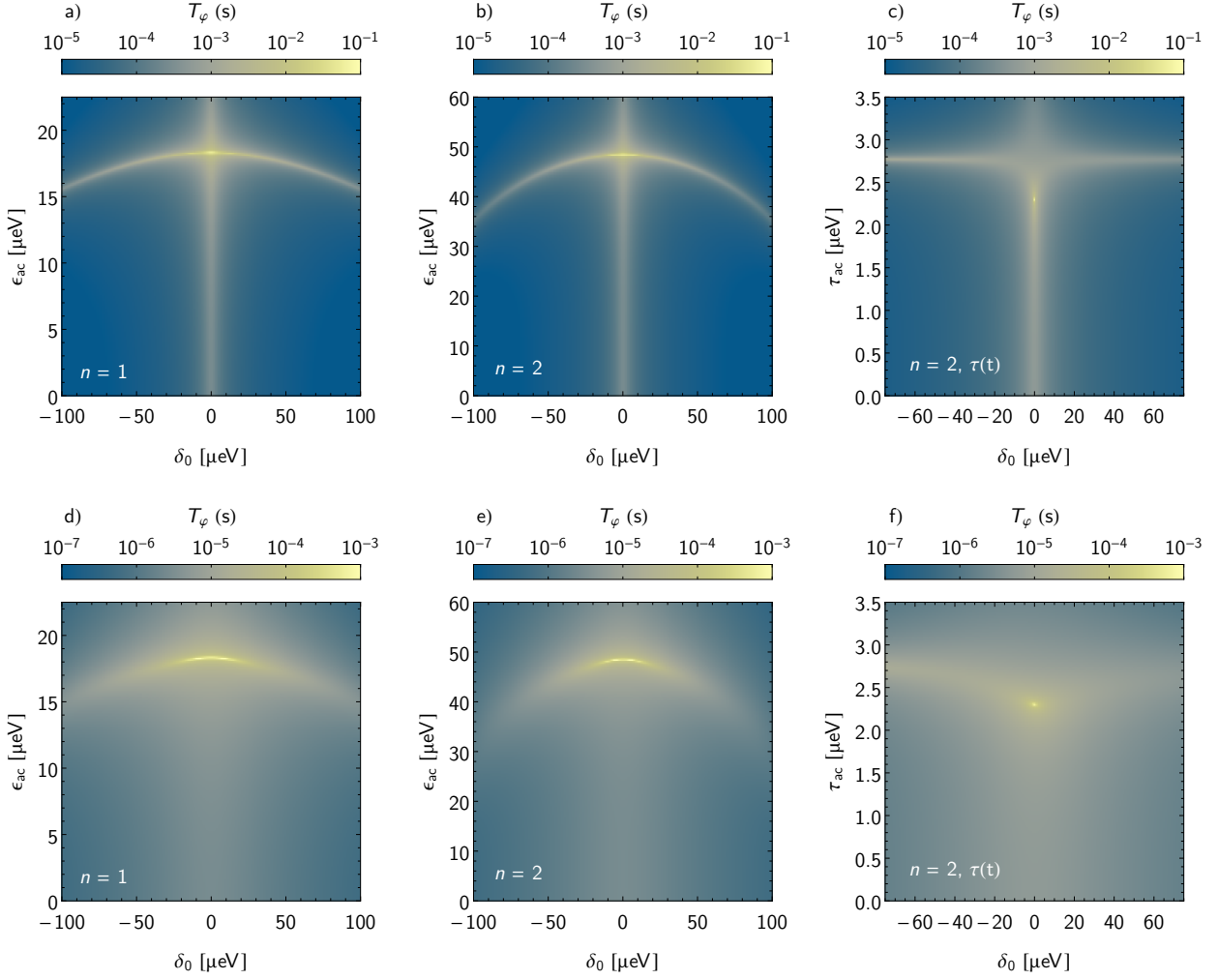


Figure 5: Dephasing time for  $\gamma = 5 \cdot 10^6$  and  $A = 10^{-6} \text{ meV}^2$  (First row, Figs. a) - c)) and  $A = 10^{-4} \text{ meV}^2$  (Second row, Figs. d) - f)). The first column (Figs a) and d)) correspond to gate driving with a one-photon resonance ( $n = 1$ ), the second column (Figs. b) and e)) to gate driving with a two-photon resonance ( $n = 2$ ) and the third column (Figs. c) and f)) to tunnel barrier driving with a two-photon resonance ( $n = 2$ ). Parameters:  $\Delta = 1.666 \mu\text{eV}$ ,  $U_1 = U_2 = 0.5 \text{ meV}$ ,  $\tau_0 = 0.01 \text{ meV}$ ,  $V = 0.1 \text{ meV}$ ,  $\gamma = 5 \cdot 10^6$ . The resonance offset is  $\delta\omega = -0.007\omega$ ,  $-0.03\omega$ , and  $-0.07\omega$  for the first, the second and the third columns, respectively.

marked, the region of longer dephasing time around  $\tau_{ac} \simeq 5 \mu\text{eV}$  is still appreciable.

## 4 Discussion

In this work we have studied the possibility of employing ac gates to engineer the properties of quantum-dot based qubits under charge noise. When quantum dot chains are driven with high ac voltage amplitudes, many sidebands become available as virtual transitions, producing new and interesting phenomena. The single photon resonance results in an exchange interaction that vanishes in the sweetspot defined in the static system and changes sign across this point. This leads to the possibility of manipulating its sign with the combined action of the dc and ac gates, and thus the ground state of the singlet-triplet qubit. Moreover, we have shown how the presence of a time-dependent voltage can produce a dynamical sweetspot, mitigating the effect of electric noise. For the two-photon resonance, we have shown that the ac voltage can be employed to induce a second order sweetspot, that is, a configuration in which both the first-order and second-order susceptibilities to electric noise are zero. In particular, we have considered the second order susceptibility of the qubit energy in a free decay model, showing that the dephasing time becomes infinite up to third order in the noise strength. We have also studied an alternative setup in which the ac driving occurs in the tunnel barrier, which provides an alternative method of controlling the exchange interaction in which it is also possible to find second-order sweetspots. These setups showcase new routes to attain high-order sweetspots through time-dependent gates, adding to previous proposals involving large tunneling amplitudes[72]. Overall, our work shows the possibilities of employing Floquet engineering to enhance the robustness of qubits in electric environments which could be generalized to other configurations, for instance for the triple quantum dot-based resonant exchange qubit. This method is within the reach of current experimental techniques.

## Acknowledgments

We acknowledge Sigmund Kohler for enlightening discussions and a critical reading of the manuscript and support from CSIC Research Platform PTI-001. G.P. acknowledges her Mercator Fellow position at CRC 1277, University of Regensburg. This work was supported by the Spanish Ministry of Economy and Competitiveness (MICINN) via Grants No. PID2020-117787GB-I00 and No. MAT-2017-86717-P.

## References

- [1] D. P. DiVincenzo, D. Bacon, J. Kempe, G. Burkard, and K. B. Whaley, *Nature* **408**, 339 (2000).
- [2] J. Levy, *Phys. Rev. Lett.* **89**, 147902 (2002).
- [3] R. Li, X. Hu, and J. Q. You, *Phys. Rev. B* **86**, 205306 (2012).
- [4] M. P. Wardrop and A. C. Doherty, *Phys. Rev. B* **90**, 045418 (2014).
- [5] M. Stopa, *Phys. B: Condens. Matt.* **249-251**, 228 (1998).
- [6] X. Hu and S. Das Sarma, *Phys. Rev. Lett.* **96**, 100501 (2006).
- [7] T. Hayashi, T. Fujisawa, H. D. Cheong, Y. H. Jeong, and Y. Hirayama, *Phys. Rev. Lett.* **91**, 226804 (2003).
- [8] D. Culcer and N. M. Zimmerman, *Appl. Phys. Lett.* **102**, 232108 (2013).
- [9] I. V. Yurkevich, J. Baldwin, I. V. Lerner, and B. L. Altshuler, *Phys. Rev. B* **81**, 121305 (2010).
- [10] O. E. Dial, M. D. Shulman, S. P. Harvey, H. Bluhm, V. Umansky, and A. Yacoby, *Phys. Rev. Lett.* **110**, 146804 (2013).
- [11] Z. Qi, X. Wu, D. R. Ward, J. R. Prance, D. Kim, J. K. Gamble, R. T. Mohr, Z. Shi, D. E. Savage, M. G. Lagally, M. A. Eriksson, M. Friesen, S. N. Coppersmith, and M. G. Vavilov, *Phys. Rev. B* **96**, 115305 (2017).
- [12] J. Schliemann, D. Loss, and A. H. MacDonald, *Phys. Rev. B* **63**, 085311 (2001).
- [13] S. D. Barrett and C. H. W. Barnes, *Phys. Rev. B* **66**, 125318 (2002).
- [14] P. Rebentrost and F. K. Wilhelm, *Phys. Rev. B* **79**, 060507 (2009).
- [15] T. Chasseur and F. K. Wilhelm, *Phys. Rev. A* **92**, 042333 (2015).
- [16] S. Mehl, H. Bluhm, and D. P. DiVincenzo, *Phys. Rev. B* **91**, 085419 (2015).
- [17] J. M. Nichol, L. A. Orona, S. P. Harvey, S. Fallahi, G. C. Gardner, M. J. Manfra, and A. Yacoby, *npj Quantum Inf.* **3**, 3 (2017).
- [18] W. Huang, C. H. Yang, K. W. Chan, T. Tanttu, B. Hensen, R. C. C. Leon, M. A. Fogarty, J. C. C. Hwang, F. E. Hudson, K. M. Itoh, A. Morello, A. Laucht, and A. S. Dzurak, *Nature* **569**, 532 (2019).
- [19] C. Kloeffer and D. Loss, *Ann. Rev. Condens. Matt. Phys.* **4**, 51 (2013), <https://doi.org/10.1146/annurev-conmatphys-030212-184248>.
- [20] Y.-P. Shim and C. Tahan, *Phys. Rev. B* **93**, 121410 (2016).



- [21] M. Russ and G. Burkard, *J. Phys.: Condens. Matt.* **29**, 393001 (2017).
- [22] A. Sala and J. Danon, *Phys. Rev. B* **95**, 241303 (2017).
- [23] A. Pan, T. E. Keating, M. F. Gyure, E. J. Pritchett, S. Quinn, R. S. Ross, T. D. Ladd, and J. Kerckhoff, *Quantum Sci. Technol.* **5**, 034005 (2020).
- [24] A. Sala, J. H. Qvist, and J. Danon, *Phys. Rev. Research* **2**, 012062 (2020).
- [25] A. Gómez-León and G. Platero, *Phys. Rev. Research* **2**, 033412 (2020).
- [26] H. Qiao, Y. P. Kandel, J. S. V. Dyke, S. Fallahi, G. C. Gardner, M. J. Manfra, E. Barnes, and J. M. Nichol, *Nat. Commun.* **12**, 2142 (2021).
- [27] M. Benito, A. Gómez-León, V. M. Bastidas, T. Brandes, and G. Platero, *Phys. Rev. B* **90**, 205127 (2014).
- [28] A. Eckardt and E. Anisimovas, *New J. Phys.* **17**, 093039 (2015).
- [29] T. Oka and S. Kitamura, *Ann. Rev. Condens. Matt. Phys.* **10**, 387 (2019).
- [30] B. Pérez-González, M. Bello, G. Platero, and A. Gómez-León, *Phys. Rev. Lett.* **123**, 126401 (2019).
- [31] G. Platero and R. Aguado, *Phys. Rep.* **395**, 1 (2004).
- [32] F. Gallego-Marcos, R. Sánchez, and G. Platero, *J. Appl. Phys.* **117**, 112808 (2015).
- [33] R. Sánchez, F. Gallego-Marcos, and G. Platero, *Phys. Rev. B* **89**, 161402 (2014).
- [34] P. Stano, J. Klinovaja, F. R. Braakman, L. M. K. Vandersypen, and D. Loss, *Phys. Rev. B* **92**, 075302 (2015).
- [35] D. Klauser, W. A. Coish, and D. Loss, *Phys. Rev. B* **73**, 205302 (2006).
- [36] D. Kim, D. R. Ward, C. B. Simmons, J. K. Gamble, R. Blume-Kohout, E. Nielsen, D. E. Savage, M. G. Lagally, M. Friesen, S. N. Coppersmith, and M. A. Eriksson, *Nat. Nanotechnol.* **10**, 243 (2015).
- [37] Y. Song, J. P. Kestner, X. Wang, and S. Das Sarma, *Phys. Rev. A* **94**, 012321 (2016).
- [38] D. M. Zajac, T. M. Hazard, X. Mi, E. Nielsen, and J. R. Petta, *Phys. Rev. Applied* **6**, 054013 (2016).
- [39] M. D. Shulman, S. P. Harvey, J. M. Nichol, S. D. Bartlett, A. C. Doherty, V. Umansky, and A. Yacoby, *Nat. Commun.* **5**, 5156 (2014).
- [40] K. Takeda, A. Noiri, J. Yoneda, T. Nakajima, and S. Tarucha, *Phys. Rev. Lett.* **124**, 117701 (2020).
- [41] A. C. Doherty and M. P. Wardrop, *Phys. Rev. Lett.* **111**, 050503 (2013).
- [42] J. M. Taylor, V. Srinivasa, and J. Medford, *Phys. Rev. Lett.* **111**, 050502 (2013).
- [43] M. Russ and G. Burkard, *Phys. Rev. B* **91**, 235411 (2015).
- [44] D. M. Zajac, A. J. Sigillito, M. Russ, F. Borjans, J. M. Taylor, G. Burkard, and J. R. Petta, *Science* **359**, 439 (2017).
- [45] M. Russ, D. M. Zajac, A. J. Sigillito, F. Borjans, J. M. Taylor, J. R. Petta, and G. Burkard, *Phys. Rev. B* **97**, 085421 (2018).
- [46] J. Jing, P. Huang, and X. Hu, *Phys. Rev. A* **90**, 10.1103/physreva.90.022118 (2014).
- [47] Y.-C. Yang, S. N. Coppersmith, and M. Friesen, *Phys. Rev. A* **95**, 062321 (2017).
- [48] A. Frees, S. Mehl, J. K. Gamble, M. Friesen, and S. N. Coppersmith, *npj Quantum Inf.* **5**, 73 (2019).
- [49] P. S. Mundada, A. Gyeenis, Z. Huang, J. Koch, and A. A. Houck, *Phys. Rev. Appl.* **14**, 054033 (2020).
- [50] Z. Huang, P. S. Mundada, A. Gyeenis, D. I. Schuster, A. A. Houck, and J. Koch, *Phys. Rev. Appl.* **15**, 034065 (2021).
- [51] Y. Makhlin and A. Shnirman, *Phys. Rev. Lett.* **92**, 178301 (2004).
- [52] J. Fei, J.-T. Hung, T. S. Koh, Y.-P. Shim, S. N. Coppersmith, X. Hu, and M. Friesen, *Phys. Rev. B* **91**, 205434 (2015).
- [53] J. Picó-Cortés, F. Gallego-Marcos, and G. Platero, *Phys. Rev. B* **99**, 155421 (2019).
- [54] A. M. Tyryshkin, S. Tojo, J. J. L. Morton, H. Riemann, N. V. Abrosimov, P. Becker, H.-J. Pohl, T. Schenkel, M. L. W. Thewalt, K. M. Itoh, and S. A. Lyon, *Nat. Mater.* **11**, 143 (2011).
- [55] M. Veldhorst, J. C. C. Hwang, C. H. Yang, A. W. Leenstra, B. de Ronde, J. P. Dehollain, J. T. Muhonen, F. E. Hudson, K. M. Itoh, A. Morello, and A. S. Dzurak, *Nat. Nanotechnol.* **9**, 981 (2014).
- [56] J. Truong and X. Hu, Decoherence of coupled flip-flop qubits due to charge noise (2021), [arXiv:2104.07485](https://arxiv.org/abs/2104.07485).
- [57] C. Zhang, X.-C. Yang, and X. Wang, *Phys. Rev. A* **97**, 042326 (2018).
- [58] H. Bluhm, S. Foletti, I. Neder, M. Rudner, D. Mahalu, V. Umansky, and A. Yacoby, *Nat. Phys.* **7**, 109 (2010).
- [59] G. de Lange, Z. H. Wang, D. Riste, V. V. Dobrovitski, and R. Hanson, *Science* **330**, 60 (2010).
- [60] D. Culcer, L. Cywiński, Q. Li, X. Hu, and S. Das Sarma, *Phys. Rev. B* **80**, 205302 (2009).
- [61] Q. Li, L. Cywiński, D. Culcer, X. Hu, and S. Das Sarma, *Phys. Rev. B* **81**, 085313 (2010).
- [62] S. Goswami, K. A. Slinker, M. Friesen, L. M. McGuire, J. L. Truitt, C. Tahan, L. J. Klein, J. O. Chu, P. M. Mooney, D. W. van der Weide, R. Joynt, S. N. Coppersmith, and M. A. Eriksson, *Nat. Phys.* **3**, 41 (2006).
- [63] C. H. Yang, A. Rossi, R. Ruskov, N. S. Lai, F. A. Mohiyaddin, S. Lee, C. Tahan, G. Klimeck,

- A. Morello, and A. S. Dzurak, *Nat. Commun.* **4**, 2069 (2013).
- [64] C. Deng, J.-L. Orgiazzi, F. Shen, S. Ashhab, and A. Lupascu, *Phys. Rev. Lett.* **115**, 133601 (2015).
- [65] A. Gandon, C. L. Calonnec, R. Shillito, A. Petrescu, and A. Blais, *Engineering, control and longitudinal readout of floquet qubits* (2021), [arXiv:2108.11260 \[quant-ph\]](https://arxiv.org/abs/2108.11260).
- [66] F. Martins, F. K. Malinowski, P. D. Nissen, E. Barnes, S. Fallahi, G. C. Gardner, M. J. Manfra, C. M. Marcus, and F. Kuemmeth, *Phys. Rev. Lett.* **116**, 116801 (2016).
- [67] G. Burkard, *Phys. Rev. B* **79**, 125317 (2009).
- [68] M. M. Ali, P.-Y. Lo, and W.-M. Zhang, *New J. Phys.* **16**, 103010 (2014).
- [69] M. Russ, F. Ginzler, and G. Burkard, *Phys. Rev. B* **94**, 165411 (2016).
- [70] G. Ithier, E. Collin, P. Joyez, P. J. Meeson, D. Vion, D. Esteve, F. Chiarello, A. Shnirman, Y. Makhlin, J. Schrieffer, and G. Schön, *Phys. Rev. B* **72**, 134519 (2005).
- [71] J. M. Taylor and M. D. Lukin, *Quantum Inf. Process.* **5**, 503 (2006).
- [72] J. C. Abadillo-Uriel, M. A. Eriksson, S. N. Coppersmith, and M. Friesen, *Nat. Commun.* **10**, 10.1038/s41467-019-13548-w (2019).
- [73] K. D. Petersson, J. R. Petta, H. Lu, and A. C. Gossard, *Phys. Rev. Lett.* **105**, 246804 (2010).
- [74] Y. Goldin and Y. Avishai, *Phys. Rev. B* **61**, 16750 (2000).

## A Effective cotunneling Hamiltonian

In this appendix, we obtain the effective cotunneling Hamiltonian of Eq. 2 starting from the full Hamiltonian for the DQD. We will consider first the case of the ac modulation in the quantum dot gate. In this case, the DQD Hamiltonian,  $\hat{H}(t)$  (Eq. 1) can be written in the interaction picture with respect to  $\hat{H}_{ac}(t)$  by a unitary transformation  $\hat{H}_I(t) = \hat{U}_I(t) [\hat{H}(t) - i\hbar\partial_t] \hat{U}_I^\dagger(t)$  where  $\hat{U}_I(t) = \exp[i\hbar^{-1} \int \hat{H}_{ac}(s) ds]$ . The transformed Hamiltonian reads  $\hat{H}_I(t) = \hat{H}_0 + \hat{H}_U + \hat{H}_{T,I}(t)$ , where

$$\hat{H}_{T,I}(t) = \sum_{\alpha,\beta;\sigma} \sum_{\nu=-\infty}^{\infty} \tau_{\nu}(t) (\hat{c}_{\alpha,\sigma}^\dagger \hat{c}_{\beta,\sigma} + \text{H.c.}), \quad (15)$$

$$\tau_{\nu}(t) = \tau J_{\nu} (\epsilon_{ac}/\hbar\omega) \exp[i\nu(\omega t + \phi)]. \quad (16)$$

The transformed tunneling term,  $\hat{H}_{T,I}(t)$ , includes all possible sideband transitions  $\tau_{\nu}(t)$  involving  $\nu$  photons, either absorbed ( $\nu > 0$ ) or emitted ( $\nu < 0$ ).

If the states with double occupancy are sufficiently separated in energy from the states in  $\mathcal{Q}$ , we may perform a time-dependent Schrieffer-Wolff transformation[53, 74] (SWT) with respect to  $H_{T,I}(t)$  in order to obtain an effective Hamiltonian for the low energy subspace  $\mathcal{Q}$ , with virtual tunneling as the leading order of perturbation, given by  $\hat{H}_{SW}(t) = e^{\hat{\Upsilon}(t)} \hat{H}_I(t) e^{-\hat{\Upsilon}(t)} - i\hbar\partial_t \hat{\Upsilon}(t)$ , where  $\hat{\Upsilon}(t) = \sum_{\sigma} s_{\beta\alpha}(t) \hat{c}_{\alpha,\sigma}^\dagger \hat{c}_{\beta,\sigma}$  is an anti-Hermitian operator and the  $s_{\alpha\beta}(t)$  satisfy

$$i\hbar\partial_t s_{\beta\alpha}(t) = \sum_{\nu=-\infty}^{\infty} \tau_{\nu}(t) - s_{\beta\alpha}(t) (\epsilon_{\alpha} - \epsilon_{\beta}). \quad (17)$$

Solving these equations together with the condition that  $s_{\beta\alpha}(t)$  is time-independent in the absence of external potentials we obtain the effective Hamiltonian. Denoting the zeroth order splitting between  $|\uparrow, \downarrow\rangle$  and  $|\downarrow, \uparrow\rangle$  as  $\Delta = E_{z,1} - E_{z,2}$ , the effective Hamiltonian in the  $\mathcal{Q} = \{|\uparrow, \downarrow\rangle, |\downarrow, \uparrow\rangle\}$  subspace is

$$\hat{H}_{SW}(t) = \begin{pmatrix} E^+(t) & \mathcal{J}^*(t) \\ \mathcal{J}(t) & E^-(t) \end{pmatrix}, \quad (18)$$

where the matrix elements are

$$\begin{aligned} E^{\pm}(t) &= \pm\Delta \\ &- 2 \sum_{\nu,\mu} \left[ \frac{\Re\{\tau_{\nu}^*(t) \tau_{\mu}(t)\}}{\delta_2 \mp \Delta - \nu\hbar\omega} + \frac{\Re\{\tau_{\nu}^*(t) \tau_{\mu}(t)\}}{\delta_1 \mp \Delta + \nu\hbar\omega} \right], \\ \mathcal{J}(t) &= \sum_{\mu,\nu} \left[ \frac{\tau_{\mu}^*(t) \tau_{\nu}(t)}{\delta_1 - \Delta + \nu\hbar\omega} + \frac{\tau_{\mu}^*(t) \tau_{\nu}(t)}{\delta_2 + \Delta - \nu\hbar\omega} \right. \\ &\quad \left. + \frac{\tau_{\nu}^*(t) \tau_{\mu}(t)}{\delta_1 + \Delta + \nu\hbar\omega} + \frac{\tau_{\nu}^*(t) \tau_{\mu}(t)}{\delta_2 - \Delta - \nu\hbar\omega} \right]. \end{aligned} \quad (19)$$

The exchange interaction is a second-order process. As a result, when an ac gate is introduced into the system, the time-dependent rate  $\mathcal{J}(t)$  involves two sideband transitions with  $\mu$  and  $\nu$  photons, respectively.  $E^{\pm}(t)$  incorporates the gradient splitting between  $|\uparrow, \downarrow\rangle$  and  $|\downarrow, \uparrow\rangle$  and a time-dependent gradient (similar to the effective ac magnetic field in EDSR). As expected,  $E^{\pm}(t) \rightarrow 0$  as  $\Delta \rightarrow 0$ , as in that case the SU(2) symmetry between the two qubit states is not broken. The case with the ac modulation in the tunneling can be obtained from this expression by taking only the sidebands with  $\mu, \nu = 0, \pm 1$ . Moreover, we note that, if both modulations of the tunneling and gate energies were present, the transformed Hamiltonian of Eq. 15 would include

two extra contributions of the form

$$\hat{H}'_{T,I}(t) = \sum_{\alpha,\beta;\sigma} \sum_{\nu} [\tau_{\nu}^{+}(t) + \tau_{\nu}^{-}(t)] (\hat{c}_{\alpha,\sigma}^{\dagger} \hat{c}_{\beta,\sigma} + \text{H.c.}), \quad (21)$$

$$\tau_{\nu}^{\pm}(t) = (\tau_{\text{ac}}/2) J_{\nu}(\epsilon_{\text{ac}}/\hbar\omega) \exp[i(\nu \pm 1)(\omega t + \phi)]. \quad (22)$$

As a result, compared to the previous case, each sideband would be further split into three, one from Eq. 15 and the two from Eq. 21.

Finally, in order to obtain the RWA Hamiltonian, a unitary transformation to the rotating frame is performed,  $\hat{H}_n(t) = \hat{U}_n(t) [\hat{H}_{\text{SW}}(t) - i\hbar\partial_t] \hat{U}_n^{\dagger}(t)$ , where  $\hat{U}_n(t) = \exp[in\omega t(\hat{S}_{z,1} - \hat{S}_{z,2})/\hbar]$  and  $n \in \mathbb{Z}$ . The two states are resonant provided that

$$\frac{1}{T} \int_0^T dt \left( \langle \uparrow, \downarrow | \hat{H}_n(t) | \uparrow, \downarrow \rangle - \langle \downarrow, \uparrow | \hat{H}_n(t) | \downarrow, \uparrow \rangle \right) = n\hbar\omega, \quad n \in \mathbb{Z}, \quad (23)$$

where  $T = 2\pi/\omega$ . The integer  $n$  denotes the order of the resonance and represents the number of photons involved in the resonant transition. The condition can be written as  $\Delta E = E^{+} - E^{-} = n\hbar\omega$ , where the mean energies  $E^{\pm}$  in the RWA are given by Eq. 4. Then, as mentioned in the main text, the oscillatory components can be neglected.

## B Corrections to the approximation

As mentioned in the main text, the SWT-based expansion up to terms  $\propto \tau^2$  is valid provided that the tunneling-widened levels are not resonant, i.e. provided that  $\tau/(\delta_1 \pm \Delta \pm \tilde{\nu}\hbar\omega) \ll 1$ . In particular, Eqs. 19-20 are valid up to factors  $\propto \tau^4$ . The next correction to  $\hat{H}_{\text{SW}}(t)$  is  $(1/2)[\hat{\Upsilon}(t), [\hat{\Upsilon}(t), \hat{H}_T(t)]]$  (which is  $\propto \tau^3$ ). This term is zero when projected to the qubit subspace  $\mathcal{Q}$ , so that the next order correction to  $\hat{H}_{\text{SW}}(t)$  is  $\propto \tau^4$ .

We may consider also what happen for larger ac voltage amplitudes (i.e. breaking the conditions detailed at the end of Sec. 3.1). Eventually, the denominators of Eq. 4 and 5 become negative for large  $\nu$  ( $> \tilde{\nu}$ ). For large ac voltage amplitudes  $\epsilon_{\text{ac}}$ , several sidebands with positive or negative denominators may interfere. This could produce a new set of dynamical sweetspots at large values of the ac voltage, in a similar way to the case of Ref. [53]. However, for the parameters considered here this results in a set of sidebands which are almost resonant, breaking the conditions for the cotunneling approximation. This results in a strong hybridization with the states in  $\mathcal{D}$ , which increases the effect of the electric fluctuations.

With respect to the RWA, the time-independent exchange rates, as obtained in Appendix A, are valid provided that  $|\mathcal{J}_n|/\hbar\omega \ll 1$ . This corresponds to a lowest-order approximation in a perturbative series in  $1/\omega$ , and its limitations have been studied in detail elsewhere[37]. Here, we follow the high frequency expansion described in Ref. [28]. After applying  $\hat{U}_n(t)$  and switching to the rotating frame<sup>2</sup>, the Hamiltonian can be written as a Fourier series  $\hat{H}_n(t) = \sum_m e^{im\omega t} \hat{H}_{n,m}$ , where the Hamiltonian of Eq. 2 is  $\hat{H}_Q^{(0)} = \hat{H}_{n,0}$ . We then have  $\hat{P}_Q \hat{H}_{n,m} \hat{P}_Q^{-1} = \Delta E_m^{(0)} \hat{\sigma}_z + \Re\{\mathcal{J}_{n,m}^{(0)}\} \hat{\sigma}_x + \Im\{\mathcal{J}_{n,m}^{(0)}\} \hat{\sigma}_y$ , where  $\hat{P}_Q$  is the projector to the qubit subspace  $\mathcal{Q}$ ,  $\Delta E_m^{(0)}$  and  $\mathcal{J}_{n,m}$  are the  $m$ th harmonics of the splitting and the exchange, respectively, from Eq. 19 and 20 after applying  $\hat{U}_n(t)$ . Then the next order correction to the RWA approximation, Eq. 2, is given by

$$\begin{aligned} \hat{H}_Q^{(1)} &= \sum_{m \neq 0} \frac{\hat{H}_{n,m} \hat{H}_{n,-m}}{m\hbar\omega} \\ &= \left[ \Delta E_n^{(1)} \hat{\sigma}_z + \Re\{\mathcal{J}_n^{(1)}\} \hat{\sigma}_x + \Im\{\mathcal{J}_n^{(1)}\} \hat{\sigma}_y \right] \end{aligned} \quad (24)$$

where

$$\begin{aligned} \Delta E_n^{(1)} &= \sum_{m=1}^{\infty} \frac{1}{2m\hbar\omega} \left( |\mathcal{J}_{n,-m}^{(0)}|^2 - |\mathcal{J}_{n,m}^{(0)}|^2 \right), \quad (25) \\ \mathcal{J}_n^{(1)} &= \sum_{m=1}^{\infty} \frac{1}{m\hbar\omega} \left( \mathcal{J}_{n,m}^{(0)} \Delta E_m^{(0)} - \mathcal{J}_{n,-m}^{(0)} \Delta E_m^{(0)} \right). \end{aligned} \quad (26)$$

The leading terms of this correction are  $\propto \tau^4/\omega$ . Since,  $\delta_1, \delta_2 \gg \hbar\omega$ , this is often of greater interest than the corrections due to the SWT. The strength of these contributions can be estimated based on these expressions to be  $\simeq |\mathcal{J}_n|/\hbar\omega \simeq 10^{-3}$  lower than the terms in Eq. 2. In any case, as seen in Eq. 24, the new terms in the expansion do not alter the way that the protocol operates.

## C The limit of small ac voltage amplitude

In this appendix, we briefly describe the  $\epsilon_{\text{ac}}/\hbar\omega \ll 1$  limit. We proceed by linearizing the expressions for  $\mathcal{J}_1$  and  $\Delta E$  (Eqs. 5 and 4, respectively). Since  $J_{\nu}(z) \simeq (z/2)^{\nu}/\Gamma(\nu+1)$  for  $z \ll 1$ , where  $\Gamma(z)$  is Euler's

<sup>2</sup>The perturbative theory of Ref. [28] provides an alternative understanding for the unitary transformation  $\hat{U}_n(t)$  described in Appendix A. The necessary condition to develop the perturbative high-frequency expansion described therein is that  $\hbar\omega$  is the largest energy scale of the system, which is accomplished by removing the splitting through  $\hat{U}_n(t)$ .

gamma function, we see that the next terms in the splitting are  $\mathcal{O}(\epsilon_{ac}^2)$ . Hence, the result is equivalent to the dc case

$$\Delta E \simeq 2\Delta \left[ 1 - \frac{2\tau^2}{\delta_2^2 - \Delta^2} + \frac{2\tau^2}{\delta_1^2 - \Delta^2} \right], \quad (27)$$

Regarding the exchange interaction, the linearized expression reads

$$\begin{aligned} \mathcal{J}_1 &\simeq \frac{\tau^2 \epsilon_{ac}}{2\hbar\omega} \\ &\times \left( \frac{1}{\delta_1 - \Delta} + \frac{1}{\delta_2 + \Delta} + \frac{1}{\delta_2 - \Delta + \hbar\omega} + \frac{1}{\delta_1 + \Delta - \hbar\omega} \right. \\ &\quad \left. - \frac{1}{\delta_2 - \Delta} - \frac{1}{\delta_1 + \Delta} - \frac{1}{\delta_1 - \Delta + \hbar\omega} - \frac{1}{\delta_2 + \Delta - \hbar\omega} \right). \end{aligned} \quad (28)$$

Taking the resonance condition to correspond exactly to  $\hbar\omega = 2\Delta$  yields the simpler expression

$$\mathcal{J}_1 \simeq \epsilon_{ac} \tau^2 \left( \frac{1}{\delta_1^2 - \Delta^2} - \frac{1}{\delta_2^2 - \Delta^2} \right). \quad (29)$$

In this limit, the RWA corresponds to ignoring (1) the dc component of  $\mathcal{J}(t)$  and (2) the counter-rotating term. The remainder of the exchange interaction is

$$\begin{aligned} e^{-i\omega t} \mathcal{J}(t) - \mathcal{J}_1 &\simeq 2e^{-i\omega t} \tau^2 \left( \frac{\delta_1}{\delta_1^2 - \Delta^2} + \frac{\delta_1}{\delta_2^2 - \Delta^2} \right) \\ &+ \frac{\epsilon_{ac} \tau^2}{\hbar\omega} e^{-i2\omega t} e^{-i\phi} \left[ \frac{\Delta}{\delta_1^2 - \Delta^2} - \frac{\Delta}{\delta_2^2 - \Delta^2} \right. \\ &\quad \left. - \frac{\Delta - \hbar\omega}{\delta_1^2 - (\Delta + \hbar\omega)^2} + \frac{\Delta - \hbar\omega}{\delta_2^2 - (\Delta + \hbar\omega)^2} \right]. \end{aligned} \quad (30)$$

Applying Eq. 24 in order to correct for these neglected terms yields a renormalization of the splitting,  $\hat{H}_Q^{(1)} \simeq \Delta E_1^{(1)} |\uparrow, \downarrow\rangle \langle \uparrow, \downarrow|$ , where

$$\begin{aligned} \Delta E_1^{(1)} &= -\frac{4\tau^4}{\hbar\omega} \left( \frac{\delta_1}{\delta_1^2 - \Delta^2} + \frac{\delta_1}{\delta_2^2 - \Delta^2} \right)^2 \\ &\quad - \frac{\epsilon_{ac}^2 \tau^4}{\hbar^3 \omega^3} \left[ \frac{\Delta}{\delta_1^2 - \Delta^2} - \frac{\Delta}{\delta_2^2 - \Delta^2} \right. \\ &\quad \left. - \frac{\Delta - \hbar\omega}{\delta_1^2 - (\Delta + \hbar\omega)^2} + \frac{\Delta - \hbar\omega}{\delta_2^2 - (\Delta + \hbar\omega)^2} \right]^2. \end{aligned} \quad (31)$$

The counter-rotating terms are  $\propto \epsilon_{ac}^2$  and as such can be neglected in this limit.

## D The limit of small gradient

In this section we describe the small gradient limit  $|\Delta|, |\nu|\hbar\omega \ll \delta_1, \delta_2$ , for all  $\nu$  which are not negligible as discussed at the end of Sec. 3.1. This is often a good approximation, since the interaction strength is the largest energy scale of the system. In that case, we can linearize the splitting (Eq. 4) to give

$$\begin{aligned} \Delta E &\simeq \Delta + 2\tau^2 \sum_{\nu=-\infty}^{\infty} J_{\nu}^2 \left( \frac{\epsilon_{ac}}{\hbar\omega} \right) \left[ \frac{1}{\delta_2} + \frac{1}{\delta_1} - \frac{1}{\delta_2} - \frac{1}{\delta_1} \right. \\ &\quad \left. - \frac{\Delta - \nu\hbar\omega}{\delta_2^2} - \frac{\Delta + \nu\hbar\omega}{\delta_1^2} - \frac{\Delta + \nu\hbar\omega}{\delta_2^2} - \frac{\Delta - \nu\hbar\omega}{\delta_1^2} \right]. \end{aligned}$$

The terms independent of  $\Delta$  are clearly zero, while the other terms are independent of the frequency, so that the Bessel function is the only factor that depends on the sideband index. Hence, we can sum over  $\nu$  to yield

$$\Delta E \simeq 2\Delta \left[ 1 - 2\tau^2 \left( \frac{1}{\delta_2^2} + \frac{1}{\delta_1^2} \right) \right], \quad (32)$$

where we have employed that  $\sum_{\nu=1}^{\infty} J_{\nu}^2(z) = (1/2) [1 - J_0^2(z)]$ . This expression is independent of the ac voltage amplitude and frequency. Regarding the exchange interaction, we have

$$\begin{aligned} \mathcal{J}_n &\simeq \tau^2 [(-1)^n - 1] \left( \frac{1}{\delta_1^2} - \frac{1}{\delta_2^2} \right) \\ &\times \left[ \sum_{\sigma=\pm 1} \sum_{\nu=\delta_{\sigma 1}}^{\infty} J_{\nu} \left( \frac{\epsilon_{ac}}{\hbar\omega} \right) J_{\nu+\sigma n} \left( \frac{\epsilon_{ac}}{\hbar\omega} \right) (\Delta + \sigma\nu\hbar\omega) \right]. \end{aligned} \quad (33)$$

As mentioned in the main text, for low gradients the odd order resonances are  $\propto \Delta$  while the resonances with  $n$  even are  $\propto \Delta^2$ .

## E Dephasing model

We consider pure dephasing in the context of a Ramsey experiment[51, 70]. We focus on the function

$$f(t) = \langle \exp(i\delta\hat{\varphi}(t)) \rangle = \exp \left( \frac{-\Delta\varphi(t)}{2} \right), \quad (34)$$

which describes the decay of coherence under the effect of longitudinal noise. Here,  $\delta\hat{\varphi}(t) = \hbar^{-1} \sum_{ij} \int_0^t ds \lambda_i(s) \hat{\xi}_j(s)$  is the accumulated phase due to a random variation of the bath operator  $\hat{\xi}_j(t)$  coupled to the system through  $\lambda_i(t)$ ,  $\langle \cdots \rangle = \text{Tr}_B \{ \cdots \hat{\rho}_B \}$ , with  $\hat{\rho}_B$  the equilibrium density matrix of the bath and  $\text{Var}[x]$  is the variance. The second equality in

Eq. 34 is obtained after expanding  $f(t)$  in terms of its cumulants[43] and assuming Gaussian noise with zero mean. We can then write  $\Delta\varphi(t)$  as a series in powers of  $A$  as

$$\Delta\varphi(t) = \Delta\varphi^{(1)}(t) + \Delta\varphi^{(2)}(t) + \dots \quad (35)$$

For the first-order coupling  $\Delta\varphi^{(1)}(t) = \text{Var}[\delta\hat{\varphi}(t)] = \langle \delta\hat{\varphi}^2(t) \rangle$ . We consider first the dephasing due to the

RWA Hamiltonian of Eq. 2

$$\begin{aligned} \Delta\varphi^{(1)}(t) &\simeq \frac{t^2}{\hbar^2} \left( \frac{\partial\omega_n}{\partial\delta_0} \right)^2 \int_{-\infty}^{\infty} d\Omega \mathcal{S}(\Omega) \text{sinc}^2\left(\frac{\Omega t}{2}\right). \\ &\simeq \frac{At^2}{2\hbar^2} \left( \frac{\partial\omega_n}{\partial\delta_0} \right)^2 \log\left(\frac{\Omega_{\text{UV}}}{\Omega_{\text{IR}}}\right). \end{aligned} \quad (36)$$

This is exactly as considered in Eq. 9 and equivalent to the free decay in the case without driving[43]. Next, we consider also all the other sidebands in Eqs. 19 and 20 (i.e. all  $\nu$  and  $\mu$ ). These yield

$$\Delta\varphi^{(1)}(t) \simeq \sum_{m,m' \neq 0} \frac{\partial F_{n,m}}{\partial\delta_0} \frac{\partial F_{n,m'}}{\partial\delta_0} \int_0^t ds e^{im\omega s} \int_0^t ds' e^{im'\omega s'} \langle \hat{\xi}_i(s) \hat{\xi}_i(s') \rangle. \quad (37)$$

If we consider that the bath dynamics are quasistatic with respect to the ac voltage dynamics, the bath operators in Eq. 37 can be assumed to be constant in time and extracted from the integral. The resulting contribution oscillates in time without decaying. This essentially divides the contribution from the oscillating terms into a low frequency part which does not contribute to dephasing and a high frequency part which describes the time scales related to the micromotion (i.e. within the ac voltage period). In particular, the contribution  $m' = -m$  acquires a form that is reminiscent of Eq. 36

$$\Delta\varphi^{(1)}(t) \simeq \frac{t^2}{\hbar^2} \sum_{m \neq 0} \frac{\partial F_{n,m}}{\partial\delta_0} \frac{\partial F_{n,\bar{m}}}{\partial\delta_0} \int_{-\infty}^{\infty} d\Omega C(\Omega - m\omega) \text{sinc}^2\left(\frac{\Omega t}{2}\right), \quad (38)$$

where  $C(\Omega) = \mathcal{S}(\Omega) + \mathcal{A}(\Omega)$  is the correlation function of the bath, with symmetric  $\mathcal{S}(\Omega)$  and antisymmetric  $\mathcal{A}(\Omega)$  components, and  $F_{n,m} = \omega_n^{-1}[\Delta E_m^{(0)}(\Delta E - n\hbar\omega) + \mathcal{J}_{n,m}^{(0)}\mathcal{J}_n]$  is the coupling constant for the contribution to dephasing of the sidebands beyond the RWA (we take the driving phase  $\phi = 0$  for simplicity). Assuming  $\Omega_{\text{UV}} + m\omega \simeq \Omega_{\text{UV}}$  and  $\Omega_{\text{IR}} + m\omega \simeq m\Omega$ , the integral for the symmetric part  $\mathcal{S}(\Omega)$  of the correlation function is given by

$$\begin{aligned} \frac{\Omega^2 t^2}{2A} \int_{-\infty}^{\infty} d\Omega \mathcal{S}(\Omega - m\omega) \text{sinc}^2\left(\frac{\Omega t}{2}\right) &= \text{Ci}(\Omega_{\text{UV}}t) - \text{Ci}(m\omega t) - \cos(m\omega t) \text{Ci}(\Omega_{\text{UV}}t) + \sin(m\omega t) \text{Si}(\Omega_{\text{UV}}t) \\ &\quad + \cos(m\omega t) \text{Ci}(\Omega_{\text{IR}}t) - \sin(m\omega t) \text{Si}(\Omega_{\text{IR}}t) + m\omega t \left[ 2\text{Si}(\Omega_{\text{UV}}t) - \frac{m\pi}{|m|} \right] \\ &\quad - m\omega t \left[ 2\text{Si}(m\omega t) - \frac{m\pi}{|m|} \right] - \frac{1}{2} [1 - \cos(m\omega t)] + \log(\gamma) - \log(\Omega_{\text{UV}}/m\Omega), \end{aligned} \quad (39)$$

where  $\text{Si}(x) = \int_0^x dy \sin(y)/y$  and  $\text{Ci}(x) = -\int_x^\infty dy \cos(y)/y$  are the sine and cosine integral functions, respectively. Assuming  $t\Omega_{\text{IR}} \ll 1$  and  $t\Omega_{\text{UV}} \gg 1$  we can employ the limit properties of these functions to reduce the problem. This yields the following expression for  $f(t)$

$$f(t) \propto \exp \left\{ - \sum_{m \neq 0} \frac{\partial F_{n,m}}{\partial\delta_0} \frac{\partial F_{n,\bar{m}}}{\partial\delta_0} \frac{A}{2(m\hbar\omega)^2} m\omega t [2\text{Si}(m\omega t) - \pi \text{sgn}(m)] \right\}, \quad (40)$$

multiplied by a series of non-decaying oscillating factors that do not contribute to dephasing. Since  $\text{Si}(x) \simeq \pi/2$  for  $x \rightarrow \infty$ , after a few periods of the ac voltage this term reduces to zero and can be neglected in the high frequency approximation. The dephasing below this time scale is  $\sim A\partial_{\delta_0}F_{n,m}\partial_{\delta_0}F_{n,\bar{m}}/(m\hbar\omega)^2$  and is regardless negligible. To reach this result we employ[43]  $\Omega_{\text{UV}}t \gg 1$  and  $\Omega_{\text{IR}}t \ll 1$ , where  $\Omega_{\text{UV}}$  and  $\Omega_{\text{IR}}$  are the ultraviolet and the infrared cutoffs, respectively, which are necessary to ensure convergence of the integral. Since we want to discuss also dephasing for longer times, we may reconsider the last condition. The next order contribution (in  $\Omega_{\text{IR}}t$ ) has



the form

$$f(t) \propto \exp \left\{ - \sum_{m \neq 0} \frac{\partial F_{n,m}}{\partial \delta_0} \frac{\partial F_{n,\bar{m}}}{\partial \delta_0} \frac{A \Omega_{\text{IR}}^2 t^2}{8 (m \hbar \omega)^2} [1 - \cos(m\omega t)] \right\}, \quad (41)$$

which exhibits the time periodic behavior that we expect from the oscillating terms and can be neglected for large frequencies. For  $\Omega_{\text{IR}} t \gg 1$  the  $\text{Ci}(x)$  function that gives rise to this behavior vanishes.

For the contribution from the antisymmetric part of the correlation function  $\mathcal{A}(\Omega) = \mathcal{S}(\Omega) \tanh(\hbar\Omega/2k_B T)$ , we consider the classical limit  $\hbar\Omega \ll 2k_B T$  first. Then we can perform a series expansion of  $\tanh(x)$  for  $x \ll 1$ . The first order term is proportional to the integral

$$t^2 \int_{-\infty}^{\infty} d\Omega \text{sinc}^2 \left( \frac{\Omega t}{2} \right) \simeq \frac{2 - 2 \cos(m\omega t)}{m\omega} - t [2\text{Si}(m\omega t) - \pi \text{sgn}(m)], \quad (42)$$

which similarly vanishes after a number of ac periods. The third order term does not contribute to dephasing, either. On the other hand, in the  $T \rightarrow 0$  limit, the result is akin to Eq. 40. Regarding the rest of the terms

$$\Delta\varphi^{(1)}(t) \simeq \sum_{m \neq m' \neq 0} \frac{\partial F_{n,m}}{\partial \delta_0} \frac{\partial F_{n,m'}}{\partial \delta_0} \int_{-\infty}^{\infty} d\Omega \mathcal{S}(\Omega) \frac{-1}{\Omega - m'\omega} \frac{1}{\Omega + m\omega} \left[ e^{-i(\Omega - m'\omega)t} - 1 \right] \left[ e^{i(\Omega + m\omega)t} - 1 \right]. \quad (43)$$

Solving the integral results in a set of constant and oscillating terms which do not contribute to dephasing in the high frequency limit, in a similar way to Eqs. 40 and 41.

The second order contribution  $\Delta\varphi^{(2)}(t)$  from the RWA Hamiltonian is given in Ref. [43] and has been included in the expression for the dephasing time in Eq. 9. The contribution from the neglected terms in Eqs. 19 and 20 due to the RWA approximation is given by

$$\Delta\varphi^{(2)}(t) \simeq \frac{1}{2} \sum_{m, m' \neq 0} \frac{\partial^2 F_{n,m}}{\partial \delta_0^2} \frac{\partial^2 F_{n,m'}}{\partial \delta_0^2} \int_0^t ds e^{im\omega s} \int_0^t ds' e^{im'\omega s'} \left\langle \hat{\xi}_i(s) \hat{\xi}_i(s') \right\rangle^2. \quad (44)$$

As for the first order, in the quasistatic limit the resulting contribution oscillates with the frequency of the voltage. As such, the main contributions to dephasing will be in the high frequency part of the correlation function. We focus on the  $m = -m'$  terms. Then, the second order contribution is

$$\Delta\varphi^{(2)}(t) = \frac{A^2}{2\hbar^2\omega^2} \sum_{m \neq 0} \frac{\partial^2 F_{n,m}}{\partial \delta_0^2} \frac{\partial^2 F_{n,\bar{m}}}{\partial \delta_0^2} I_m^{(2)}(t), \quad (45)$$

$$I_m^{(2)}(t) = \frac{\omega^2 t^2}{A^2} \int_{-\infty}^{\infty} d\Omega \int_{-\infty}^{\infty} d\Omega' C(\Omega) C(\Omega') \text{sinc}^2 \left[ \frac{(\Omega + \Omega' + m\omega)t}{2} \right]. \quad (46)$$

Similarly, the  $m \neq -m'$  terms are

$$\Delta\varphi^{(2)}(t) = \frac{A^2}{2\hbar^2\omega^2} \sum_{m \neq m' \neq 0} \frac{\partial^2 F_{n,m}}{\partial \delta_0^2} \frac{\partial^2 F_{n,m'}}{\partial \delta_0^2} K_{m,m'}^{(2)}(t), \quad (47)$$

$$K_{m,m'}^{(2)}(t) = \frac{-\omega^2}{A^2} \int_{-\infty}^{\infty} d\Omega \int_{-\infty}^{\infty} d\Omega' C(\Omega) C(\Omega') \frac{\left[ e^{-i(\Omega + \Omega' - m'\omega)t} - 1 \right]}{\Omega + \Omega' - m'\omega} \frac{\left[ e^{i(\Omega + \Omega' + m\omega)t} - 1 \right]}{\Omega + \Omega' + m\omega}. \quad (48)$$

For the estimation of these integrals we resort to numerical integration. We have represented the integral  $I_m^{(2)}(t)$  in Fig. 6 a). The behavior of the integral can be separated in a region  $t \ll \omega^{-1}$  ( $m\omega = 1$  GHz in this case) where the behavior is similar to the quasistatic case, with a limiting dependence  $\propto -t^2$  as in Eq. 36 (represented with a dashed black line in the figure), an intermediate regime with  $t \sim \omega^{-1}$  where the integral oscillates and a long time behavior as  $t \gg \omega^{-1}$  which is dominated by the low frequency behavior of the integral and does not contribute to dephasing. Hence, as discussed for Eq. 40, we expect that in the high-frequency regime the dephasing due to these second-order terms can also be neglected for time scales larger than the ac bias. We have also represented the integral  $K_{m,m'}^{(2)}(t)$  in Fig. 6 b) for  $m' = 3m$ . In this case, most of the contribution is constant in the regime

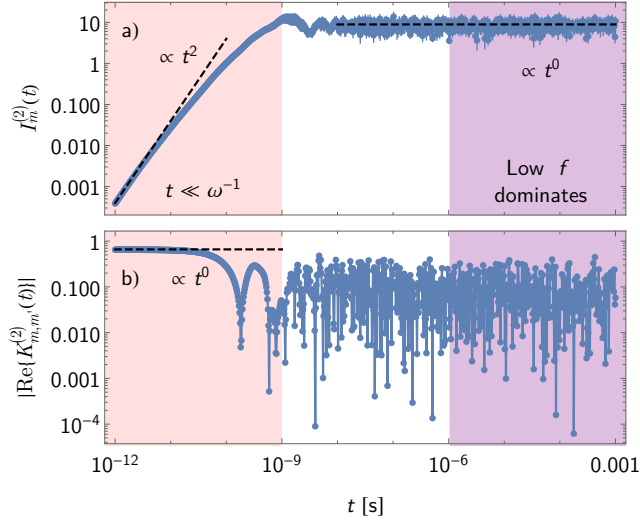


Figure 6: a) Integral  $I_m^{(2)}(t)$  contributing to dephasing for  $m = -m'$  (See Eq. 46.) as a function of time for  $T = 40$  mK,  $m\omega = 1$  GHz,  $\Omega_{\text{IR}} = 10^3$  Hz and  $\Omega_{\text{UV}} = 1$  THz (error bars reflect integration errors in the quasi-Monte Carlo approach employed to calculate them). b) Integral  $K_{m,m'}^{(2)}(t)$  contributing to the dephasing time for  $m \neq -m'$  (See Eq. 48.) for the same parameters as a, with  $m' = 3m$ .

$t \ll \omega^{-1}$ . We remark that these contributions to the accumulated phase include both the effect of noise on the time evolution during the micromotion and the higher order corrections to the RWA Hamiltonian (e.g. Eq. 24).